

Mechanisms of Sinoatrial Pacemaker Synchronization: A New Hypothesis

Donald C. Michaels, Edward P. Matyas, and Jose Jalife

A model of electrically coupled sinus node cells was used to investigate pacemaker coordination and conduction. Individual cells were simulated using differential equations describing transmembrane ionic currents. Intrinsic cycle lengths (periods) were adjusted by applying constant depolarizing or hyperpolarizing bias current, and cells were coupled through ohmic resistances to form two-dimensional arrays. Activation maps of 81–225 coupled cells showed an apparent wavefront conducting from a leading pacemaker region to the rest of the matrix even though the pattern actually resulted from mutual entrainment of all spontaneously beating cells. Apparent conduction time increased with increasing intercellular resistance. Appropriate selection of pacemaker cycle lengths and intercellular resistances permitted the accurate simulation of the activation sequence seen experimentally for the rabbit sinus node. Furthermore, a simulated acetylcholine pulse applied to a randomly selected 20% of the cells in this model produced a pacemaker shift that lasted several beats. These results support the hypothesis that sinus node synchronization occurs through a “democratic” process resulting from the phase-dependent interactions of thousands of pacemakers. (*Circulation Research* 1987;61:704–714)

Normal pacemaking in the mammalian heart depends on the coordinated discharge frequency of thousands of pacemaker cells comprising the sinoatrial (SA) region. Indeed, coordinated behavior is essential to generate rhythmic activity and produce a single impulse with each cardiac cycle, but the mechanisms leading to this behavior are poorly understood.

Various mechanical and electrical schemes have been proposed. Mechanical hypotheses suggest that coordination depends either on stretch exerted directly by one cell on another^{1,2} or on an indirect mechanical response to the systolic pulse wave in the sinus node artery.³ Mechanically induced synchronization of pacemakers has not been completely ruled out but is not widely accepted.⁴ On the other hand, the recent demonstration of gap junctions in the sinus node^{5,6} has led to the suggestion that electrical coupling underlies pacemaker synchronization. Two modes of electrical synchronization have been proposed. Under one scheme, a cell, or small group of cells, would serve as the “dominant” pacemaker, and all other intrinsically active pacemakers in the node would be driven by the dominant pacemaker to fire at its faster intrinsic frequency. A second hypothesis suggests that the synchronization of sinus pacemaker activity may be a more “democratic” process whereby the individual

cells, each beating at slightly different intrinsic frequencies, mutually interact via electrical coupling to achieve a “consensus” as to when to fire.^{7,8}

Our recent experiments^{8–10} and computer simulations¹¹ of coupled sinus node cells provide support to the “democratic consensus” hypothesis. Moreover, those results suggest that cell-to-cell interactions leading to mutual entrainment may indeed form the basis for the synchronization of pacemaker activity in the whole sinus node. We report the results of studies with two-dimensional arrays or “sheets” of SA cells, which indicate that a variety of phenomena including synchronization, impulse conduction, pacemaker shifts, and various SA arrhythmias may be explained on the basis of the phase-dependent mutual interactions of individual SA cells. Preliminary accounts of these simulations have appeared elsewhere in abstract form.^{12,13}

Materials and Methods

Simulations of SA pacemaker activity were carried out using the model of Yanagihara and coworkers¹⁴ to describe membrane potential as a function of individual membrane ionic currents. Programs were written in FORTRAN and run on a PDP 11/73 computer (Cyberchron Corp., Garrison, N.Y.) equipped with a VT125 (Digital Equipment Corp., Marlboro, Mass.) and a Tektronix 4010 graphics terminal (Tektronix Inc., Beaverton, Ore.). Results of the computer runs were stored on hard disk or magnetic tape for later analysis. Hard copy was generated with a Tektronix Model 4631 Hard Copy Unit or a Hewlett-Packard Model 7470A plotter (Waltham, Mass.). Some computations were performed on computer facilities at the New York State Center for Advanced Technology in Computer Applications and Software Engineering (CASE Center) at Syracuse University and at the Cornell National Supercomputer Facility, Ithaca, N.Y.

From the Departments of Pharmacology and Physiology SUNY/Health Science Center at Syracuse, N.Y.

Supported by National Institutes of Health grant HL 29439, NSF grant DMB 8612770, and by Grants-in-Aid from the American Heart Association, with funds provided in part by the Upstate New York and Broome County New York Chapters. Dr. Jalife is an Established Investigator of the American Heart Association.

Address for correspondence: Dr. Donald C. Michaels, Department of Pharmacology, SUNY/Health Science Center, 766 Irving Avenue, Syracuse, NY 13210.

Received September 15, 1986; accepted May 29, 1987.

Single-Cell Model

Reconstruction of the membrane potential of a single SA cell was done as previously described in detail.^{11,15} Briefly, the model consists of membrane ionic currents in parallel with a membrane capacitance of $1 \mu\text{F}/\text{cm}^2$. Membrane surface area for a single cell is assumed to be 1 cm^2 . Time- and voltage-dependent membrane currents include a slow inward current, a sodium current, a potassium current, and a hyperpolarization-activated current. In addition, there is a time-independent "leak" current. A modified Euler method¹⁶ was used for integration of the equations. Since there are no extremely rapid current changes in the sinus node model, an integration time step of 1.0 msec was used for all simulations. Stability of the model was checked by comparison with results obtained at a time step of 0.05 msec . In several tests of this type, there were no significant differences in results. Initial starting conditions were obtained by running the unperturbed model for 20 consecutive spontaneous beats and storing the gating variables and membrane potential for the 20th beat in 1% increments of the cycle length. Subsequent simulations could then be started at any point in the natural cycle. In analysis programs, a voltage greater than -20 mV was assumed to signal firing of the pacemaker.

Provisions were made in the single-cell model for various perturbations. Programs allowed for the addition of constant hyperpolarizing or depolarizing bias current so as to alter intrinsic pacemaker frequency.¹¹ Additional equations describing a separate acetylcholine (ACh)-activated potassium channel¹⁷ were added to the model to allow for the simulation of brief ACh ("vagal") pulses.

Models of Coupled Cells

Sinus node activation was simulated by connecting individual cells as diagrammed schematically in Figure 1. The procedure used is a logical extension of that previously described for coupling two cells.¹¹ Briefly, the current from one cell to its neighbor is derived from Ohm's law as the difference in their potential divided by the "intercellular" coupling resistance (all extracellular resistances are assumed to be negligible). This current is then added to membrane ionic currents before integration. Each cell thus has a current contribution

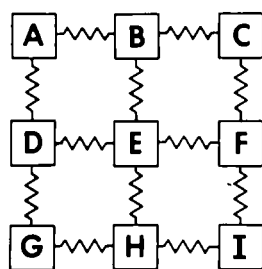


FIGURE 1. Diagram illustrating the arrangement of coupling resistances between simulated pacemaker cells in a bidimensional matrix.

from its neighbor. Rescaling of the simulation results to biologic proportions is relatively straightforward. For all simulations except those dealing with modeling of the rabbit sinus node (Figure 5), element dimensions of $1.0 \times 1.0 \times 0.2 \text{ mm}$ and a surface-to-volume ratio of $5,000 \text{ cm}^{-1}$ can be assumed. For a 15×15 array, the dimensions would be $1.5 \times 1.5 \text{ cm}$ with a thickness of $200 \mu\text{m}$ and a surface area (volume \times surface-to-volume ratio) for each element of 1.0 cm^2 . From the value for specific resistivity in the sinus node of $2,000 \Omega \cdot \text{cm}$,¹⁸ the intercellular resistance in ohms can be calculated as $2,000/0.02$, or $100 \text{ k}\Omega$. In the case of the simulations of the rabbit sinus node, dimensions of $0.5 \times 0.5 \times 0.5 \text{ mm}$ were chosen for individual elements such that the overall dimensions ($0.75 \times 0.75 \times 0.05 \text{ cm}$) were similar to those of the rabbit sinus node.⁶ When a surface-to-volume ratio of $8,000 \text{ cm}^{-1}$ is assumed, cell surface area is 1 cm^2 . Under these conditions, intercellular resistance (assuming again the value of $2,000 \Omega \cdot \text{cm}$ for specific resistivity calculates to $40 \text{ k}\Omega$. These values are in reasonable agreement with data obtained under experimental conditions. More than 2 cells can be coupled in a two-dimensional lattice, with each cell connected by a resistor to every one of its neighbors (Figure 1). A given cell interacts with 2, 3, or 4 of its immediate neighbors depending on its position. Cells in corners (A, C, G, and I) will be influenced by only 2 neighbors, those on the sides (B, D, F, and H) by 3, and those in the middle (E) by 4. To maintain symmetry during the computation, coupling currents are calculated for all elements before the membrane potential of any cell of the array is changed. The value of any of the coupling resistances can be specified individually, but, typically, all are set to the same value.

For large arrays, the sequential display of membrane potential yields little useful information about the behavior of the sheet. Figure 2 shows the procedure used for those cases. In panel A, the model consists of a 9×9 array. For this particular example, normal cells surround a group of 4 faster (shaded) cells whose intrinsic frequency was increased by applying bias depolarizing current.¹¹ Intercellular coupling resistance was set to an intermediate value ($350 \text{ k}\Omega$; specific resistivity is $7,000 \Omega \cdot \text{cm}$), and the program was run to simulate 6 seconds of interaction. Panel B shows the traces for all cells of the array aligned sequentially. Thus, the first 9 traces are from the 9 cells in the first row (from left to right), the second 9 traces from the cells in the second row, and so on. Coordinated behavior is present with all cells firing at a common period. Yet, the "wavy" overall nature of this panel suggests that the pacemakers are not all firing at the same time. This is also illustrated by a pseudo-ECG (Figure 2C), where the first derivative of the mean membrane potential is plotted as a function of time. Since all cells were programmed to fire together initially, the first peak of the ECG is tall and narrow. As the discrepancy in firing time increases, upward

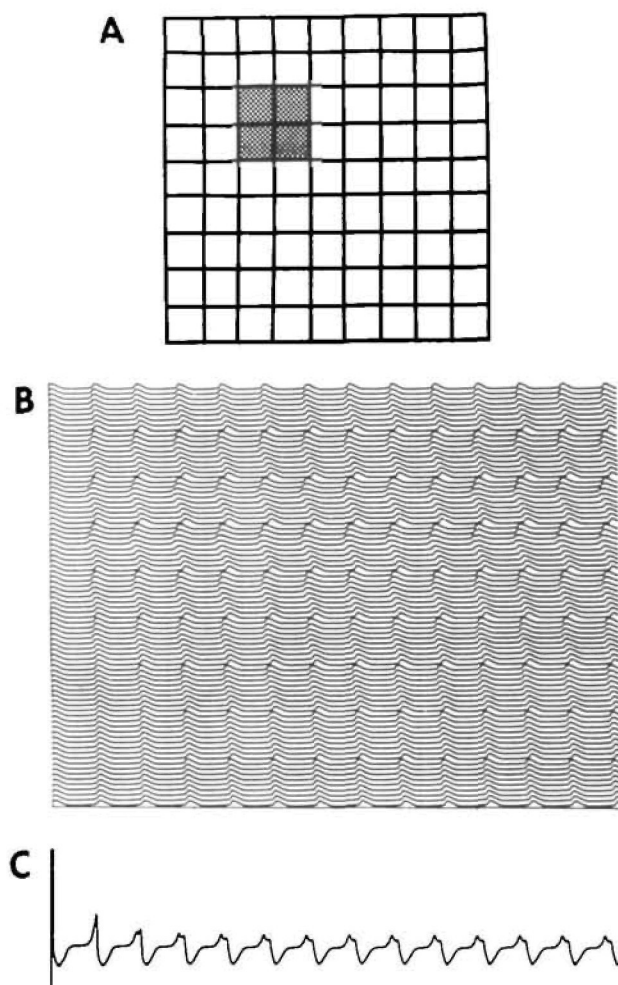


FIGURE 2. *Mutual entrainment in a 9×9 two-dimensional matrix of simulated sinus node cells. Panel A, model arrangement. All cells were capable of beating spontaneously. Four cells (shaded) had a shorter intrinsic period (238 msec) than the rest of the pacemakers (318 msec). Panel B, membrane potentials of all 81 cells arranged in rows from top to bottom. Top trace corresponds to the cell in the top row, first column (from left to right) of the matrix. Ninth trace is from the cell in the top row, last column, etc. All traces begin at the same phase, i.e., when membrane potential is -20 mV. Cells mutually entrained in a 1:1 manner to a common cycle of 300 msec. However, cells did not all fire simultaneously, as indicated by the wavy nature of panel B. Panel C, ECG generated by plotting the first derivative of the mean membrane potential for all cells vs. time. Peaks indicate firings of the entire sheet and are lower in amplitude and wider when individual cell firing times are more disperse.*

deflections decrease in amplitude and widen. Peak height is, thus, a measure of the relative number of cells firing synchronously. The interval between upward peaks is a measure of the cycle length for the whole preparation. Taller, narrower peaks indicate simultaneous depolarization, while smaller, wider peaks indicate dispersion of depolarization; downward peaks are indicators of repolarization. Of note, this is not entirely analogous to an electrogram signal that

would be recorded from an electrode above the model surface since the spatial contributions of net membrane currents are not considered. It does, however, represent a simple indicator of average activity within the sheet.

Color activation mapping was used to further analyze the behavior of the sheet models. Under this scheme, a given "block" corresponding to a cell position in the matrix is assigned a color representing its relative firing time. In Figure 3, the boxes labelled A, B, C, and D in the upper left represent individual cells connected by resistors. The traces in the upper right show the membrane potentials for each of the cells during a run at a relatively low value of coupling resistance (100 k Ω ; specific resistivity is 2,000 Ω ·cm). Note that while the pacemakers are mutually entrained in a 1:1 fashion, they do not all fire at the same time. The traces in the lower right panel show a fragment of the upper traces on an expanded scale. The time at which the first cell fires in each beat is taken as time zero. Different colors are then assigned to each subsequent 10- or 20-msec time interval. When the membrane potential of a given cell exceeds a specified value indicating that it has fired, its corresponding position block is assigned the color associated with that time interval. Thus, if the firing of cell A is taken as time zero, its position block (lower left panel, top left corner) is assigned the color red. Cell B fires in the yellow time interval, and its position block is assigned the color yellow, and so on. The resulting activation map (lower left panel) indicates the relative firing time of each cell in its proper position in the array, and its method of preparation is similar to that used to prepare maps from multiple recordings of sinus node⁶ and atrium.¹⁹

Simulation Protocols

Three types of simulation protocols were used for the present studies. In all three, cells were coupled as

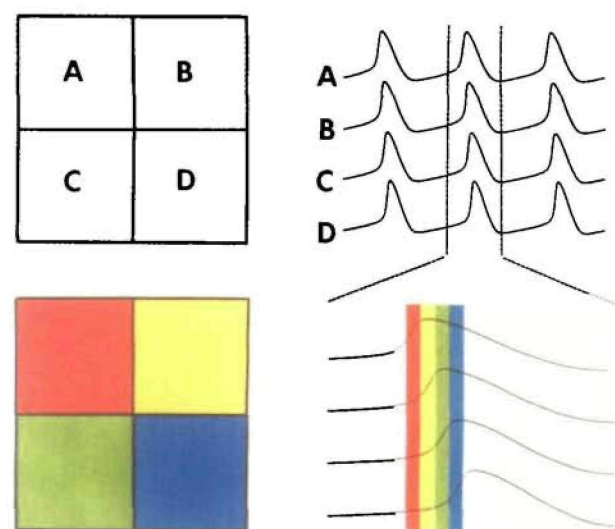


FIGURE 3. *Construction of a color activation map in a 2×2 matrix of mutually entrained sinus pacemaker cells.*

described above. Differences lay in the number and distribution of cells with altered intrinsic cycle length (period, 1/frequency). In initial runs, a small group of cells in the middle of the sheet was assigned a higher intrinsic period (by the application of bias depolarizing current), while those cells surrounding it had normal intrinsic cycle lengths of 318 msec.

In a more advanced version of the model, different intrinsic periodicities were assigned (by adding bias depolarizing or hyperpolarizing current) to regions of a large array. The matrix consisted of a small higher frequency central portion surrounded by normal cells. A strip of inexcitable cells (those where all active inward ionic currents had been removed and only the potassium and leak currents were left) was positioned to the right of the high frequency group. The entire border of the array was populated with lower frequency cells.

In a final version, a model of the "compact" region of the sinus node was used.⁶ A class of 10 pacemaker types with different intrinsic cycle lengths ranging from 290 to 390 msec was produced by applying specific amounts of bias depolarizing or hyperpolarizing current. One of the cell types (and thus intrinsic cycle lengths) was then assigned to each of the cells of a 15×15 array at random, resulting in a uniform distribution of cell types.

For a given run in each version, coupling resistances

between cells were all set to the same level, and values for membrane potential, individual ionic currents, coupling currents, and total membrane current were computed and stored. Coupling resistance was increased systematically in subsequent runs until 1:1 mutual entrainment was lost. Action potential values including cycle lengths and firing times for each cell of the array were stored during a run, and a separate program was used to assign colors for the activation maps for each beat (where beat is defined as that time interval during which all cells fire). Color activation maps were then prepared for those beats of interest.

Results

Achievement of Stable Patterns

The model illustrated in Figure 2A was used for the initial studies designed to investigate the effects of coupling resistance on mutual entrainment. A central group of 4 cells with a slightly higher intrinsic frequency (intrinsic period, 238 msec) as a result of bias depolarizing current ($-0.5 \mu\text{A}/\text{cm}^2$) was surrounded by cells to which no bias current was applied (intrinsic period, 318 msec). Specific resistivity between all cells of the array was set to a common value for a given computer run. Figure 4 summarizes results obtained at 3 different specific resistivities (panel A, 1,000; panel B, 2,000; panel C, 4,000 $\Omega\cdot\text{cm}$). Traces to the right in each panel indicate the first derivative of the mean

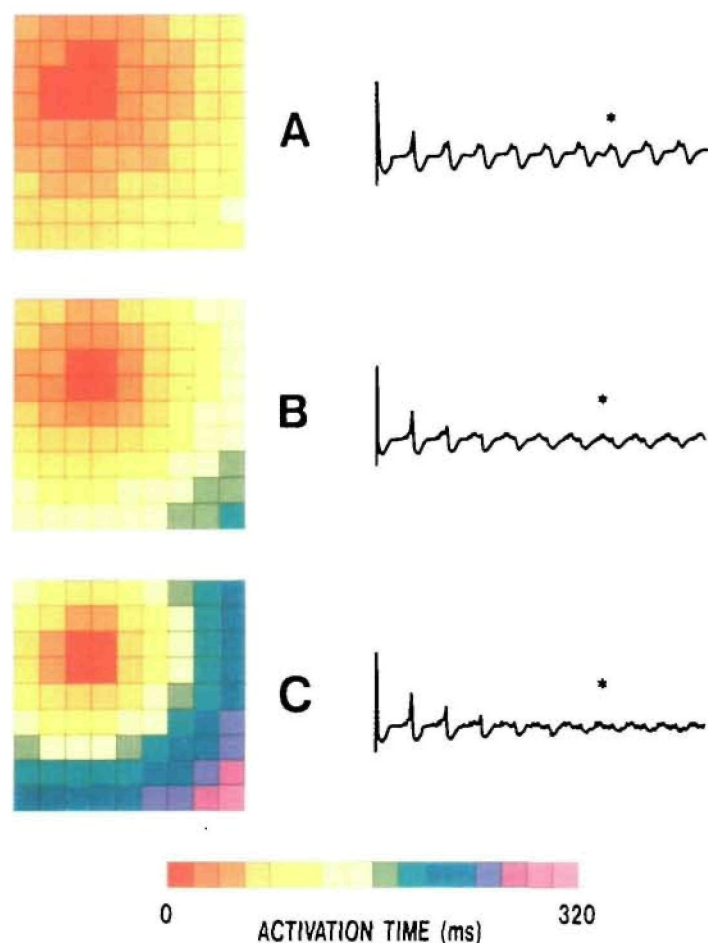


FIGURE 4. Color activation maps and ECG traces showing effects of coupling resistance on pattern of mutual entrainment. Same model as in Figure 2A. ECGs to the right show development of stable entrainment patterns and relative degree of synchronization as a function of time. Activation maps to the left correspond to single beats indicated by the asterisks on respective ECGs. Colors indicate time of firing of each cell (see color code in bottom panel) in relation to that of the earliest to fire during that beat. Cell dimensions are $100 \times 100 \times 20 \mu\text{m}$; specific resistivities are 1,000, 2,000, and 4,000 $\Omega\cdot\text{cm}$ for panels A, B, and C, respectively.

membrane potential for all elements of the sheet (ECG). These traces show that several beats were required for stabilization of the pattern of 1:1 mutual entrainment. During this stabilization period, there was a progressive widening and decrease in amplitude of the major peak associated with each beat. The interval between major peaks represents the cycle length of individual beats. Steady-state conditions were determined by noting when the activation pattern and the cycle length of the mutually entrained (1:1) pattern (as measured by the times between responses) did not change. This usually occurred by the eighth beat. Cycle lengths for beats after stabilization had been achieved showed a progressive decrease as coupling resistance was increased (cycle lengths were 300, 290, and 285 msec for A, B, and C, respectively).

Mutual Entrainment and Apparent "Conduction"

At each of the levels of coupling resistance, the individual color maps prepared for a single beat (asterisks) indicate both the position and activation time of every cell in the sheet with respect to the earliest cell to fire within that beat (see "Materials and Methods"). This cell was assigned time zero, and any cell that fired within the initial 0–19 msec was assigned the color red. Additional colors were used to designate activation times in 20-msec increments (see color code in bottom panel). In Figure 4A (left panel; specific resistivity, $1,000 \Omega \cdot \text{cm}$), once a stable 1:1 mutual entrainment had been achieved, the earliest cells to fire in a given beat were those with the higher intrinsic frequency. Activation times then increased with distance from this region. The activation pattern thus shows apparent conduction spreading radially from a central region even though it actually results from the mutual entrainment of all of the pacemakers in the array, rather than from continuous propagation from a faster dominant pacemaker region. Additional support for this notion comes from the observation that the frequency at which the array entrains (period, 300 msec) is not the same as that of the faster cells but somewhere intermediate between the intrinsic periods of the two cell types (238 and 318 msec).

At the higher coupling resistances (Figure 4B and 4C), there were increases in apparent conduction times as might be expected in the sinus node when the degree of cell-to-cell coupling is reduced.^{9,10} This is also evident in the ECG traces as a widening of the complexes and by the appearance of subpeaks associated with individual beats. Of interest in the activation map of panel C is the fact that the last cell to fire in a given beat activates only several milliseconds before the earliest discharge in the next beat. This is suggestive of a pattern similar to atrial flutter where there is successive activation of all elements such that, at any given time, at least one element of the array is active.

Modelling of Rabbit Sinus Node

In a recent study, Bleeker et al⁶ used microelectrodes to prepare activation maps for the sinus node region of rabbit atrium. They noted a radial spread of activation

from a dominant pacemaker region in the central portion of the SA node and a subsequent spiraling of the wavefront around a narrow band of tissue with apparently lower excitability located in the "free wall" border of the node and running parallel to the crista terminalis. Microelectrode recordings obtained from cells in this zone showed what appeared to be active responses with slow upstrokes and "notched" morphologies. They attributed these responses to local summation of propagated action potentials originating in neighboring cells at either side of the low excitability zone. Before that study, Sano and Yamagishi²⁰ had noted the existence of such a zone. Since the more recent experiments of Bukauskas et al¹⁸ indicate that there are no abrupt changes of intercellular resistivity in the rabbit SA region, it can be safely assumed that the most likely mechanism for conduction impairment is an altered excitability of cells within this narrow band of tissue.

In an attempt to simulate the complicated activation pattern of the rabbit sinus node, we used the bidimensional matrix shown in the top portion of Figure 5, which consisted of 15×15 cells for a total of 225. As in the model shown in Figure 4, 4 cells in the center were forced to discharge at a relatively brief cycle length (302 msec). Most other active cells in Figure 5 had an intrinsic period of 318 msec. However, to mimic more closely the normal pacemaker hierarchy of the node in that species,^{21–23} the pacemakers in all 4 borders of the sheet were slightly hyperpolarized for an intrinsic period of 358 msec. Finally, to simulate the conditions of low excitability in a narrow band,⁶ all 11 cells colored black (Figure 5, top panel) were made inexcitable by deleting all active inward currents (slow inward, sodium and hyperpolarization-activated). In the absence of coupling, these cells had a stable resting potential of -40 mV and were incapable of generating any kind of active responses but could be depolarized by their neighbors when conditions of low-resistance coupling were allowed.

The resulting map illustrated in the bottom panel of Figure 5 clearly demonstrates that, at the appropriate value of common coupling resistance (40 k Ω), the model can reproduce very accurately the activation pattern of the rabbit SA node (Bleeker et al,⁶ see their Figure 1). Again, as a result of the electrotonic interactions among all cells, there is a stable pattern of 1:1 entrainment to a cycle length of 328 msec (not shown) with apparent conduction from a central pacemaker region to the periphery. However, in this case, the dominant pacemaker region is displaced toward the left, and the intrinsically fastest cells are in the rightmost part of this region. This occurs because the inexcitable zone exerts a tonic current load on these cells with a concomitant slowing effect. In addition, the activation sequence in the map is such that, as in the experimental preparation,⁶ all cells at the left of the inexcitable zone activate within the first 40 msec. Furthermore, since the inexcitable zone forms an additional resistive barrier to the mutual interactions between the faster cells and the right side of the sheet,

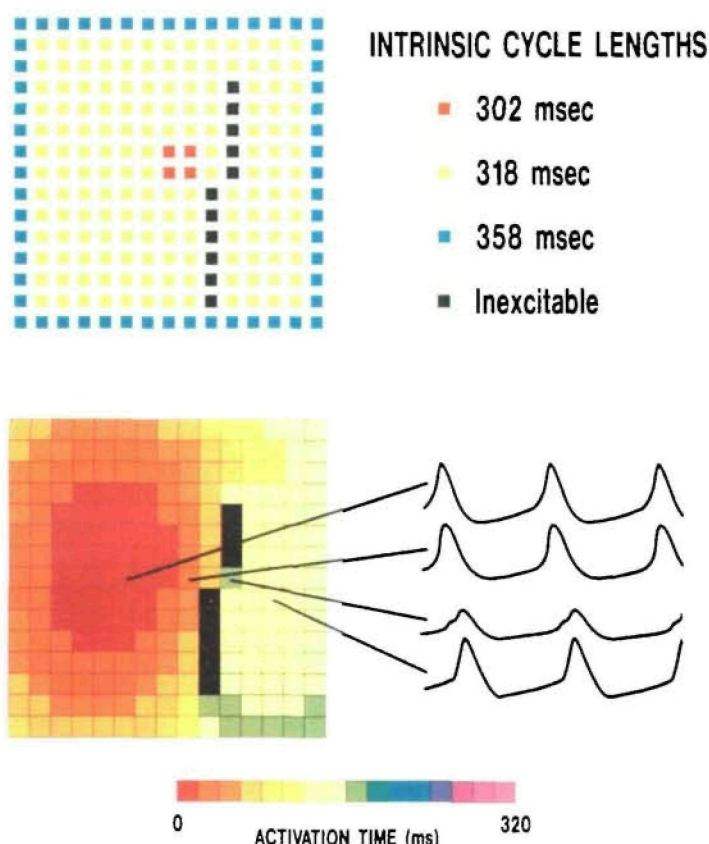


FIGURE 5. Model of rabbit sinus node consisting of 15×15 array pacemaker cells. Cell dimensions are $50 \times 50 \times 50 \mu\text{m}$; specific resistivity, $2,000 \Omega \cdot \text{cm}$; surface-to-volume ratio is $8,000 \text{ cm}^{-1}$. Top panel, location of cells with different intrinsic frequencies. Inexcitable cells have no active inward membrane currents. Lower left panel, activation map after 10 beats of mutual 1:1 entrainment at an axial resistance of $40 \text{ k}\Omega$. Colors indicate time of firing of each cell (see color code at the bottom). The resulting conduction pattern is similar to that obtained experimentally by Bleeker et al.⁶ Lower right panel, membrane potential traces for selected cells (connecting lines).

the activation front appears to circumvent the superior margin of the black zone, reaching the inferior right border with an apparent delay of 70–80 msec.

Traces to the right of the activation map (Figure 5) show membrane potentials of 4 cells of the array. Black lines indicate the positions of the cells from which the traces were obtained. Note their sequential activation in accordance with data presented in the map. In addition, there were rhythmic repetitive depolarizations in the inexcitable cell as a result of the summated electrotonic spread from neighboring cells. These notched responses are similar to those observed by Bleeker et al⁶ in experimental studies, which they attributed to summation of active events in excitable but depressed cells.

Compact Region of the Sinoatrial Node

Previous studies^{6,21} have indicated that the central or compact region of the SA node is the site of earliest activation and is comprised of approximately 5,000 pacemaker cells. A generalized view regarding the nature of the synchronization in the node is that there is a dominant or “master” pacemaker cell or pacemaker center within this region. When this master cell or center fires, all other cells are activated by the propagated suprathreshold event. To investigate our alternative hypothesis that such synchronization may in fact arise from the mutual entrainment of all SA pacemaker cells, we attempted to simulate the conditions that we believe should prevail in this compact zone.

For this version of the model, each pacemaker within

the compact region was assumed to have an intrinsic periodicity that is slightly different from that of its neighbors. Thus, cells in a 15×15 matrix were randomly assigned 1 of 10 intrinsic periods (ranging from 290 to 390 msec). We then investigated the effects of coupling resistance on the pattern of activation resulting from the mutual interaction of the cells. As shown in Figure 6 (A1, B1, and C1), when there were no interactions (i.e., no coupling), the activation maps were quite random in appearance. The remaining maps illustrate the time-dependent development of fixed phasic relations and stable 1:1 mutual entrainment at two different levels of coupling resistance. When the degree of cell-to-cell coupling was relatively strong (specific resistivity, $400 \Omega \cdot \text{cm}$; middle panels), dominant pacemaker regions were apparent by the second beat (A2). By beat 4 (B2), the size of most of the pacemaker regions had been reduced, and a single dominant region (upper right in B2) had begun to emerge. With time, the pattern became stable, and only a single pacemaker region remained by beat 8 (C2). Note that dominant regions appeared to cluster on edges or in corners of the sheet. This is presumably due to a “boundary condition” resulting from the fact that cells in these areas are influenced by fewer neighbors (see “Discussion”). When the pattern had stabilized, there was apparent conduction from the dominant region to other regions of the sheet.

As seen in the bottom panels of Figure 6, when the specific resistivity was increased ($2,000 \Omega \cdot \text{cm}$), the coexistence of two dominant regions was observed (see map in C3), although the larger region remained in the

same position as seen before. Again, pacemaker centers tended to cluster in corners and apparent conduction was also observed. However, as might be expected from a condition of weak coupling, there was a considerable increase in apparent conduction time, and the interval between beats (i.e., the cycle length of the entire sheet) decreased as coupling resistance was increased. This phenomenon has been observed previously in both experimental¹⁰ and mathematical¹¹ studies.

The obvious conclusion of the results with the random distribution of pacemakers in the sheet model is that mutual entrainment, in which individual cells exhibit reciprocal, phase-dependent electrotonic interactions with their neighbors, can give rise to coordination of the entire population, and mimic the conditions that prevail when a leading pacemaker group activates the rest of the cells with a delay.

Pacemaker Shift Induced by an Acetylcholine Pulse

An additional test for the validity of the model is that it should be able to reproduce behavioral patterns of the node in response to external perturbations. It is well

known that vagal stimulation can induce shifts in the location of the dominant pacemaker region.^{24,25} These pacemaker shifts are probably due to the inhomogeneous nature of the vagal innervation within the node^{26,27} as well as to the differing sensitivities of the various cell types to the hyperpolarizing effects of ACh.^{28,29} Experimental studies have also shown that vagally induced pacemaker shifts can occur not only from the center to the periphery but also within the central region itself.²⁹ The possibility that our model may simulate the behavior of the experimental preparation was investigated.

To mimic the conditions of vagal stimulation, after a given pattern of activation had been established, the specific ACh-activated potassium current was turned on (see "Materials and Methods") for a brief time (ACh pulse of 100-msec duration) in a random 20% of cells. The activation maps presented in Figure 7 illustrate results obtained when coupling was established at a specific resistivity of 400 $\Omega \cdot \text{cm}$. The matrix on the left shows the control activation sequence during the third beat. As usual, the cells had already selected a dominant pacemaker region (in red), although rela-

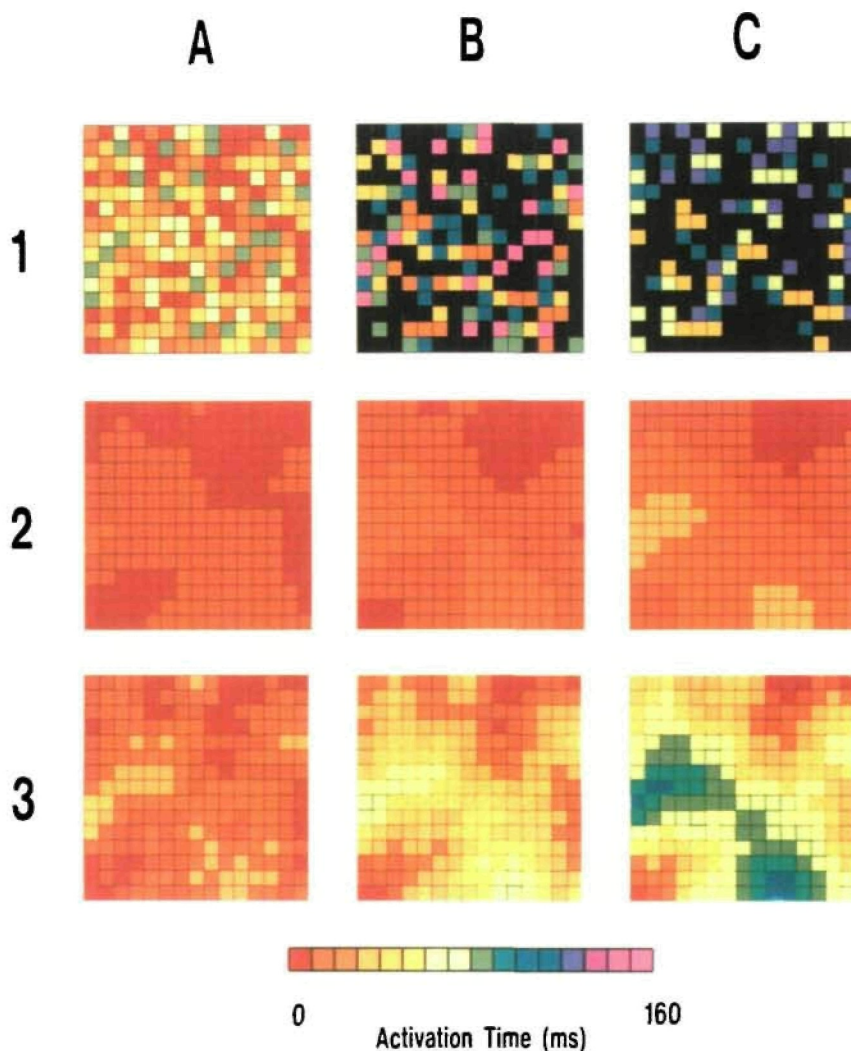


FIGURE 6. Effects of electrical coupling on synchronization in a 15×15 matrix of pacemakers simulating the compact region of the sinus node. Cell dimensions, $100 \times 100 \times 20 \mu\text{m}$; surface-to-volume ratio, $5,000 \text{ cm}^{-1}$. Intrinsic cycle lengths from 290 to 390 msec were assigned at random. Color activation maps are shown for single beats (2, 4, and 8) during 3 runs at different levels of coupling. The patterns in the top panels (A1, B1, and C1) show the randomness of activation when common coupling resistance was infinite. Since this randomness precluded activation mapping based on a beat by beat analysis, panels B1 and C1 represent firing times of cells within the first 160 msec (see color code at bottom) relative to beats 4 and 8 of the lower panels. Cells in black did not fire during this interval. In the middle and bottom panels, the specific resistivity was set to 400 and 4,000 $\Omega \cdot \text{cm}$, respectively. In both cases, stable 1:1 mutual entrainment developed with one region (in red) phase-leading the rest of the sheet. In the middle panels (A2, B2, and C2), at the lower value of specific resistivity, entrained cycle length is 322 msec (not shown), and apparent propagation time eventually becomes stable at 40 msec (C2). In the bottom panels (A3, B3, and B3), at specific resistivity of 4,000 $\Omega \cdot \text{cm}$, entrained cycle length is shorter (318 msec); apparent propagation is heterogeneous and much prolonged.

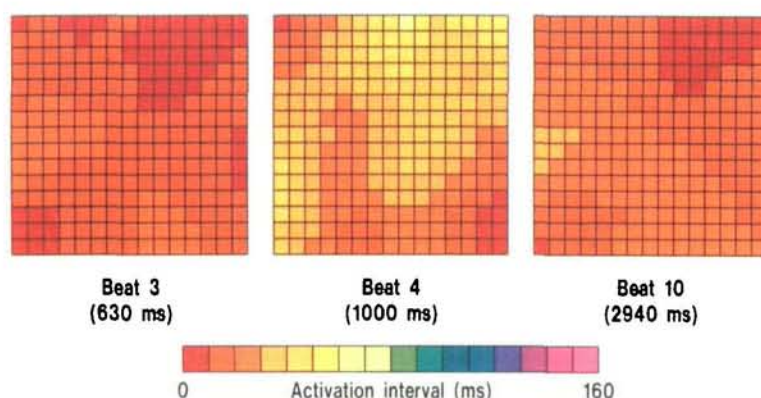


FIGURE 7. Pacemaker shift induced by ACh pulse. Cell dimensions, surface-to-volume ratio, and distribution of intrinsic frequencies were the same as in Figure 6; specific resistivity was $400 \Omega \cdot \text{cm}$. Numbers under each matrix indicate time of run at which map was obtained. An ACh pulse ($1 \times 10^{-6} \text{ M}$, 100-msec duration) was applied to a randomly selected 20% of cells 150 msec after the earliest firing during beat 3, i.e., 780 msec after the simulation run was started.

tively small areas of early activation persisted outside that region at this time. Between beats 3 and 4, a 100-msec ACh pulse ($1 \mu\text{M}$) was applied simultaneously to 20% of cells, 150 msec after the earliest discharge in the third beat. Immediately thereafter (beat 4), there was a shift of dominance to the lower right corner, and a significant increase in the apparent conduction time. These effects, however, did not persist, and by the tenth beat (right), dominance had returned to its original site with a total apparent conduction time that was similar to control.

Both the ACh-induced shifting of the site of earliest activation and the increase in apparent conduction time have been observed in experimental preparations.^{25,28} The tendency of the pacemaker site to cluster in corners is again apparent and probably results from the boundary restrictions inherent in the model. Finally, the ACh pulse produced a transient lengthening of the overall period of the sheet from 315 msec during beat 3 to 370 msec during beat 4 and back to 318 msec at beat 10. This, too, is in accord with experimental observations.^{29,30}

The results of these simulations supply additional evidence to support our hypothesis that the synchronization of the sinus node is mediated by the mutual entrainment of the multiple pacemakers of this region. Not only can synchronization be achieved, but it responds appropriately to various perturbations including increases in coupling resistance and ACh pulses.

Discussion

The Sinus Node as an Oscillator Population

The major result of this study is the demonstration that the SA node behaves like a large population of electrically coupled oscillators (pacemakers) with differing intrinsic periodicities. The dynamic interactions among cells in such a population give rise to activation patterns that mimic the spread of excitation from a dominant center to the periphery, even though the pattern actually results from mutual entrainment of large numbers of spontaneously beating cells. This represents a major departure from the classic view of the sinus node as a slowly conducting tissue in which the action potential, initiated by a small cluster of dominant pacemaker cells, propagates radially at an accelerating pace. Under such a scheme, the SA rate and rhythm would be determined by the activity of that

leading center, which would overdrive latent pacemaker cells and force them to fire at its command. In contrast, our computer simulations indicate that sinus node coordination may actually be a dynamic process whereby all pacemaker cells contribute to the establishment of the rhythm. Under these conditions, the pacing rate is not that of the intrinsically fastest pacemaker but is determined by the tonic and phasic electrotonic interactions and by the degree of electrical coupling among all cells.¹¹ Furthermore, our computerized simulations demonstrate that many of the phenomena seen in sinus nodal tissues under experimental conditions can be explained in terms of the mutual entrainment scheme.

Mutual Entrainment as the Basis of Apparent Conduction

Various experimental^{8-10,31} and theoretical^{11,32-34} models have been used to study interactions between coupled cardiac pacemakers. In all cases, the reciprocal influence of the firing of one pacemaker on the periodicity of another is phase dependent, and the magnitude of this influence is a function of the degree of electrical coupling between the cells. Consequently, 2 pacemaker cells can achieve mutual entrainment and fire at a common period that may be different from the intrinsic cycle length of either cell. These observations formed the basis of our hypothesis that the electrically coupled pacemaker cells of the SA node might coordinate (i.e., synchronize) their activity by such a mechanism. In the present study, it was determined that under a variety of initial conditions, whenever electrical coupling provided for sufficient interaction, large numbers of pacemakers with different intrinsic frequencies could mutually entrain to a common period. Yet, although the resulting pattern of activity showed that all pacemakers were discharging at the same frequency, their activation time was usually not simultaneous. Indeed, as predicted by oscillator theory and demonstrated by previous studies of biologic oscillators⁷ and cardiac pacemaker activity,^{8,35} the process of mutual entrainment requires that there be some phase difference between the oscillators for coordination to be maintained. In our sheet models, activation maps showed that there was always some dispersion of activation times, which was manifest as an apparent wavefront propagating radially from a

leading pacemaker center to the periphery. The apparent conduction time depended on the value of the common coupling resistance and the relative numbers of cells with any given intrinsic cycle length.

It has been demonstrated that agents (e.g., ouabain) capable of increasing intercellular coupling resistance can produce an increase in SA conduction time.¹⁰ Our simulations with bi-dimensional matrixes of coordinated sinus pacemakers also showed an apparent slowing of conduction when coupling resistance was increased. This suggests that many sinus nodal rhythm disturbances usually attributed to slowing of intranodal conduction may in fact be explained in terms of alterations of electrical coupling and loss of stable mutual entrainment of spontaneously beating cells.

Simulation of the Rabbit Sinus Node

A number of electrophysiologic and anatomic studies have demonstrated that the sinus node is a nonhomogeneous structure,^{6,36,37} and many of those studies have suggested the existence of a hierarchy of spontaneous activity in the node, depending on cell location as well as on the species.^{6,38,39} In the rabbit, dominant pacemaker activity is usually attributed to the compact region, which contains about 5,000 cells that are characterized by a relatively low maximum diastolic potential, slow-response action potentials, and a smooth transition from diastolic depolarization to action potential upstroke.^{5,20} Outside of this region, membrane potential becomes gradually more negative, slow diastolic depolarization becomes less steep and upstroke velocity increases.^{6,40} Such inhomogeneities have been attributed to regional anatomic and electrophysiologic differences of the various cell types, and recent ultrastructural studies have revealed a gradual transition in cell type from the compact region to the periphery of the node.^{6,22,23}

The present version of our model is simplistic in the sense that it does not incorporate atrial tissue at the boundaries of the node, and it does not consider the existence of anisotropy¹⁸ as well as regional differences in gap junctional distribution and cell-to-cell coupling.^{6,41} As noted above (see "Materials and Methods"), scaling of our simulations to a biologic proportion gave similar values for coupling resistance to those used by Joyner et al.⁴² Furthermore, there is little information regarding actual coupling resistance in the sinus node. Nevertheless, the wide ranges of coupling resistance encountered in our previous studies (1–200 k Ω corresponding to specific resistivities of 20–4,000 $\Omega\cdot\text{cm}$; Michaels et al¹¹) for 1:1 entrainment of two coupled pacemakers with different intrinsic periodicities agree with the values of intracellular resistivity calculated by Bukauskas et al¹⁸ for the isolated rabbit sinus node. Indeed, these investigators estimated this value to be in the range of 2,000–4,000 $\Omega\cdot\text{cm}$ when measured perpendicularly to the crista terminalis. In addition, one has to consider the fact that when the difference in intrinsic frequencies in a system of two coupled pacemaker cells is not too large (i.e., ≤ 100 msec; Michaels et al¹¹), 1:1 entrainment can be

maintained for a coupling resistance of 200 k Ω or greater. Hence, the values of specific resistivity (400–4,000 $\Omega\cdot\text{cm}$ for networks of 15×15 cells) at which we have studied 1:1 entrainment at progressively longer "apparent" conduction times in our multiple cell networks represent a reasonable, though conservative, approximation of the degree of electrical coupling in a biologic preparation of sinus node tissues. Indeed, by appropriate choice of cell types (i.e., intrinsic frequencies or excitability) and their arrangement in the matrix, it was possible to simulate very accurately the pattern of activation seen when the whole sinus node of the rabbit was mapped with microelectrodes.⁶ At first glance, it might be somewhat surprising that the activity of such a complex structure could be simulated so readily with a primitive model incorporating relatively few (225) pacemaker elements. Yet, it should be borne in mind that light microscopy studies³⁶ have indicated that pacemaker cells in the sinus node tend to group in small clusters separated from other clusters by a thick basement membrane and connected to them only at discrete points. If one assumes that pacemakers within each cluster are relatively well coupled, one could further assume that each cell within the matrix in our model represents one of these clusters. Indeed, as shown in voltage clamp studies,⁴³ segments of rabbit sinus node as much as 0.2–0.3 mm in diameter are isopotential and behave as single cells. Hence, to the extent that the equations of Yanagihara et al¹⁴ can mimic very accurately behavioral patterns of single cells or cell clusters,⁴³ the model presented in Figure 5 can be viewed as a faithful macroscopic representation of the normal activation sequence in the isolated rabbit SA node.

The shift of the site of earliest activation to a region other than that of cells with highest intrinsic frequency (Figure 5) is somewhat analogous to the experimental observations of Kodama and Boyett.²² These authors studied regional differences by first mapping the rabbit sinus node to determine the site of earliest activation. They then dissected this tissue into small ball-like segments that corresponded to the central, transitional, and peripheral areas of the node. Each of the segments retained spontaneous activity, which is in accordance with the idea that the sinus node consists of electrically coupled multiple pacemakers. In addition, they found that the segment with the highest intrinsic frequency was from a region close to the crista terminalis, several millimeters away from the site of earliest activation in the intact node. Although the results of that study should be interpreted with some caution because of the possibility of cell damage during the dissection procedure, the presumed basis for the shift of the dominant pacemaker region is the hyperpolarizing influence of atrial cells near or within the crista terminalis on the cells with the intrinsically faster rate of discharge (see also Joyner and Van Capelle⁴¹). Our simulations did not include atrial cells or the crista terminalis. Yet, the presence of the inexcitable zone to the right of the intrinsically fastest cells in the matrix (Figure 5) served

as a tonic hyperpolarizing influence on these cells and slowed their approach to threshold. The final effect was to shift the site of earliest activation to an intrinsically slower pacemaker site, thus supporting the interpretation given by Kodama and Boyett²² to their experimental results.

The appearance of notched waveforms in cells rendered inexcitable by removal of their active current components is also the result of the electrotonic influence of neighboring cells and reproduces very accurately experimental results.⁶ Cells on either side of the line of inexcitability activate at considerably different times, and, thus, their added electrotonic manifestation in the inexcitable cells gives rise to what appears to be action potentials with a characteristic notch. Similar activity has been seen in both experimental and mathematical studies of two pacemakers acting through an intermediary inexcitable cell.⁹

Additional simulations incorporating larger numbers of elements with differing intrinsic frequencies as well as regional differences in cell-to-cell coupling, atrial cells at the boundaries, and an inexcitable region at the free-atrial-wall boundary of the node should give us an even more accurate picture of the activation patterns. Moreover, such simulations should provide testable predictions regarding the dynamic electrotonic interactions of the sinus pacemakers with their surroundings and the mechanisms of intranodal and SA conduction disturbances.

Boundary Conditions

In simulations of the central or compact region of the sinus node, the dominant pacemaker site that emerged when the cells were mutually entrained tended to be located in a corner of the sheet (Figure 6). Even under conditions where there was a pacemaker shift, the location of the new pacemaker was in a corner. This was attributed to a kind of boundary problem since the cells on the edges or in the corner of the sheet have fewer neighbors to influence their activity (Figure 6). Further investigation of this issue was possible by connecting the cells located on opposite sides of the sheet (i.e., top to bottom and left to right) to form a torus. Even though the structure of the sinus node does have certain boundary conditions and is more analogous to a sheet than to a torus, it was of interest to determine whether a dominant pacemaker that emerged under these circumstances would remain in one place or wander over the whole unbounded surface. Preliminary results with the SA node torus (not shown) suggest that once stable conditions have been achieved after 4–5 beats, the leading pacemaker does not wander but remains at a specific site from which the impulse appears to spread radially at a velocity that depends on the coupling resistance among elements.

Pacemaker Shift Induced by Acetylcholine Pulse

ACh or vagally induced pacemaker shifts have been observed to occur most often from the central region to the periphery of isolated sinus node preparations,²⁵ but they also occur within the central region itself.²⁹

Application of a brief ACh pulse in our model of the compact region reproduces very accurately what is seen experimentally with vagal stimulation, not only by shifting the site of earliest activation to a different part of the matrix, but also by slowing the apparent conduction time. Pacemaker shifts within the node have been attributed to several mechanisms including possible regional differences in ACh-receptor density,²² differing sensitivity of the various cell types to the hyperpolarizing effects of ACh,^{28,29} and regional differences in the tissue content of catecholamines.²² Our previous simulations with the Yanagihara model suggest that the balance of inward versus outward transmembrane currents during diastole in a given cell may in fact determine the sensitivity to an external perturbation. Indeed, whether it be in response to a brief ACh pulse¹⁵ or a hyperpolarizing or depolarizing current pulse,¹¹ sensitivity is lower in cells having characteristics of “true” pacemakers (i.e., those with less negative membrane potential and higher intrinsic frequency) than in so-called “latent” pacemaker cells. Furthermore, the fact that in the present simulations, only a randomly selected 20% of the cells had the ACh pulse applied suggests that a similar mechanism may be involved in the biologic preparation since it has been shown that the distribution of cholinergic terminals within this tissue is quite heterogeneous.²⁷ Finally, although not shown, larger ACh pulses (ACh concentrations up to 10^{-5} M and durations up to 250 msec) were noted to prolong the duration of the pacemaker shift, which is also in accordance with experimental observations.²⁵

Conclusions

From the results of our simulation studies with the two-dimensional sheet, several conclusions can be drawn. The sinus node can be modelled as a population of electrically coupled pacemakers with differing intrinsic frequencies. Pacemaker dominance and apparent conduction in the node may be the result of a democratic consensus achieved through mutual entrainment of multiple pacemaker cells. Shifts of dominance induced by ACh or vagal stimulation can be explained on the basis of transient perturbation of phasic interactions and mutual entrainment of pacemakers. Mathematical modelling can be a useful tool to study the normal and abnormal electrophysiologic properties of the sinus node.

Acknowledgments

We thank Mario Delmar and Irwin M. Weiner for reading the manuscript, and Joanne Scheible for technical assistance. Additional computational support was provided by the New York State Center for Advanced Technology in Computer Applications and Software Engineering (CASE Center) at Syracuse University and by the Cornell National Supercomputer Facility that is supported in part by the National Science Foundation, New York State, and IBM Corporation.

References

1. Jensen D: *Intrinsic Cardiac Rate Regulation*. New York, Appleton-Century-Crofts, 1971, pp 163–194
2. Pollack GH: Cardiac pacemaking: An obligatory role of catecholamines? *Science* 1977;196:731–738
3. James TN: Pulse and impulse in the sinus node. *Henry Ford Hosp Med J* 1967;15:275–299
4. Sperelakis N: Propagation mechanisms in heart. *Annu Rev Physiol* 1979;41:441–457
5. Masson-Pevet M: The fine structure of cardiac pacemaker cells in the sinus node and in tissue culture (thesis). University of Amsterdam, The Netherlands
6. Bleeker WK, Mackaay AJC, Masson-Pevet M, Bouman LN, Becker AE: Functional and morphological organization of the rabbit sinus node. *Circ Res* 1980;46:11–22
7. Winfree AT: *The Geometry of Biological Time*. New York, Springer-Verlag, 1980, pp 115–118
8. Jalife J: Mutual entrainment and electrical coupling as mechanisms for synchronous firing of rabbit sino-atrial pace-maker cells. *J Physiol (Lond)* 1984;356:221–243
9. Delmar M, Jalife J, Michaels DC: Effects of changes in excitability and intercellular coupling on synchronization in the rabbit sino-atrial node. *J Physiol (Lond)* 1986;370:127–150
10. Takayanagi K, Jalife J: Effects of digitalis intoxication on pacemaker rhythm and synchronization in the rabbit sinus node. *Am J Physiol* 1986;250:H567–H578
11. Michaels DC, Matyas EP, Jalife J: Dynamic interactions and mutual synchronization of sinoatrial node pacemaker cells. *Circ Res* 1986;58:706–720
12. Michaels DC, Matyas EP, Jalife J: Pacemaker shifts induced by acetylcholine (ACh) pulses in a mathematical model of the sinus node (abstract). *Fed Proc* 1986;45:771
13. Michaels DC, Matyas EP, Jalife J: A study of mutual entrainment as a mechanism of synchronization in the sinus node (abstract). *Biophys J* 1986;49:272A
14. Yanagihara K, Noma A, Irisawa H: Reconstruction of sinoatrial node pacemaker potential based on the voltage clamp experiments. *Jpn J Physiol* 1980;30:841–857
15. Michaels DC, Matyas EP, Jalife J: A mathematical model of the effects of acetylcholine pulses on sinoatrial pacemaker activity. *Circ Res* 1984;55:89–101
16. Randall JE: *Microcomputers and Physiological Simulation*. Reading, Mass, Addison-Wesley Publishing Co, Inc, 1980, pp 1–235
17. Osterrieder W, Noma A, Trautwein W: On the kinetics of the potassium channel activated by acetylcholine in the SA node of the rabbit heart. *Pflugers Arch* 1980;386:101–109
18. Bukauskas FF, Gutman AM, Kisunas KJ, Veteikis RP: Electrical cell coupling in rabbit sino atrial node and atrium: Experimental and theoretical evaluation, in Bouman LN, Jongsma HJ (eds): *Cardiac Rate and Rhythm*, The Hague, Martinus Nijhoff, 1982, pp 195–214
19. Allesie MA, Lammers WJEP, Bonke FIM: Intra-atrial reentry as a mechanism for atrial flutter induced by acetylcholine and rapid pacing in the dog. *Circulation* 1984;70:123–135
20. Sano T, Yamagishi S: Spread of excitation from the sinus node. *Circ Res* 1965;26:423–430
21. Sano T, Sawanobori T, Adaniya H: Mechanism of rhythm determination among pacemaker cells of the mammalian sinus node. *Am J Physiol* 1978;235:H379–H384
22. Kodama I, Boyett MR: Regional differences in the electrical activity of the rabbit sinus node. *Pflugers Arch* 1985;404:214–226
23. West A, Belardinelli L: Correlation of sinus slowing and pacemaker shift caused by adenosine in sinus node. *Pflugers Arch* 1985;403:75–81
24. Meek WJ, Eyster JAE: Experiments on the origin and propagation of the impulse in the heart. IV. The effect of vagal stimulation and of cooling on the location of pacemaker within the sino-auricular node. *Am J Physiol* 1914;34:368–383
25. Bouman LN, Gerlings ED, Biersteker PA, Bonke FIM: Pacemaker shift in the sino-atrial node during vagal pacemaker stimulation. *Pflugers Arch* 1968;302:255–267
26. Nonidez J: The structure and innervation of the conductive system of the heart of the dog and Rhesus monkey, as seen with a silver impregnation technique. *Am Heart J* 1943;26: 577–597
27. James TN: Cardiac innervation: Anatomic and pharmacologic relations. *Bull NY Acad Med* 1967;43:1041–1086
28. Toda N, West T: Changes in sino-atrial node transmembrane potentials on vagal stimulation of the isolated rabbit atrium. *Nature* 1965;205:808–809
29. Spear JF, Kronhaus KD, Moore EN, Kline RP: The effect of brief vagal stimulation on the isolated rabbit sinus node. *Circ Res* 1979;44:75–88
30. Jalife J, Slenter VAJ, Salata JJ, Michaels DC: Dynamic vagal control of pacemaker activity in the mammalian sinoatrial node. *Circ Res* 1983;52:642–656
31. Veenstra RD, DeHaan RL: Electrotonic interactions between aggregates of chick embryo cardiac pacemaker cells. *Am J Physiol* 1986;250:H453–H463
32. Berkinblit MB, Kalinin DI, Kovalev SA, Chailakhyan LM: Study with the Noble model of synchronization of the spontaneously active myocardial cells bound by a highly permeable contact. *Biofizika* 1975;20:121–125
33. Torre V: A theory of synchronization of heart pace-maker cells. *J Theor Biol* 1976;61:55–71
34. Ypey DL, VanMeerwijk VOM, Ince C, Groos G: Mutual entrainment of two pacemaker cells. A study with an electronic parallel conductance model. *J Theor Biol* 1980;86:731–755
35. Ypey DL, Clapham DE, DeHaan RL: Development of electrical coupling and action potential synchrony between paired aggregates of embryonic heart cells. *J Membr Biol* 1979; 51:75–96
36. James TN: The sinus node. *Am J Cardiol* 1977;40:965–986
37. Tranum-Jensen J: The fine structure of the atrial and atrioventricular (AV) junctional specialized tissues of the rabbit heart. in Wellens HJJ, Lie KI, Janse MJ (eds), *The Conduction System of the Heart*. Leiden, Stenfert Kroese BV, 1976 pp 51–81
38. James TN, Sherf L, Fine G, Morales AR: Comparative ultrastructure of the sinus node in man and dog. *Circulation* 1966;34:139–163
39. Boineau JP, Schuessler RB, Mooney CR, Wylds AC, Miller CB, Hudson RD, Borremans JM, Brockus CW: Multicentric origin of the atrial depolarization wave — The pacemaker complex. *Circulation* 1978;58:1036–1048
40. Seyama I: Characteristics of the rectifying properties of the sino-atrial node cell of the rabbit. *J Physiol (Lond)* 1976; 255:379–397
41. Joyner RW, Van Capelle FJL: Propagation through electrically coupled cells: How a small SA node drives a large atrium. *Biophys J* 1986;50:1157–1164
42. Joyner RW, Picone J, Veenstra R, Rawling D: Propagation through electrically coupled cells: Effects of regional changes in membrane properties. *Circ Res* 1983;53:526–534
43. Noma A, Irisawa H: Membrane currents in the rabbit sinoatrial node as studied by the double microelectrode method. *Pflugers Arch* 1976;364:45–52

KEY WORDS • sinus node • pacemaker shift • mutual entrainment • mathematical models • sinoatrial conduction • acetylcholine